J Electroceram (2008) 21:815–818
DOI 10.1007/s10832-008-9503-5

Preparation and characterization of ZnSe nanocrystals in silica gel-glasses

Minqiang Wang · Xiao Huo · Xi Yao · Kui Yang · Haiyan Hao · Xing Wan

Received: 23 May 2005 / Accepted: 28 August 2005 / Published online: 29 April 2008

Abstract Transparent $ZnSe/SiO_2$ nanocomposites were prepared using a sol–gel technique which was followed by a reductive thermal treatment. The several approaches for avoiding the aggregation of ZnSe nanocrystals (NCs) doped in silica gel-glass were presented and adopted compositely during the preparation process. Transmission electron microscopy (TEM), X-ray diffraction (XRD), UV–Vis optical absorption, and Raman scattering were used to study the microstructural properties of the nanocomposites. All nanocomposites were found to show significant finite size effects as characterized by the broadened XRD peaks, blueshifts of the interband optical absorption edge, and the asymmetric broadening of the Raman scatterings. The structure and properties were correlated and discussed.

Keywords ZnSe · Nanocrystals · Gel-glasses · Nanocomposite

1 Introduction

Recently, there has been extensive interest in synthesizing nanocomposites by dispersing the nanocrystals (NCs) in silica glass due to the enhanced optical, electrical, and magnetic properties [1, 2]. The physical properties of the nanocomposite are mainly dominated by the quantum size effect of NCs, which can change radically the electronic structures of the materials. A key to the property tailoring is to explore new nanocomposite methodologies. Several methods have been developed to fabricate nanocomposite structures, including sol–gel [3], supersaturated glass solution [4], RF-sputtering [5], pulsed laser deposition [6] and so on. All these techniques allow a deep understanding of the quantum size effects of the well dispersed nanoparticles.

Several methods are used to characterize the nanoparticle size of gel–glass nanocomposite, including transmission electron microscopy (TEM), X-ray diffraction pattern (XRD), optical absorption, Raman scattering and etc. TEM is a direct characterization method which is suitable to observe nanoparticle shapes and distribution. The other three methods (XRD, Absorption and Raman) belong to the indirect survey methods that involve the light diffraction, quantum dot confinement and phonon confinement effects, respectively. A lot of papers have reported the preparation of gel–glass nanocomposites [7], however the microstructure of the gel–glass nanocomposites are barely reported using both direct and indirect characterization method at one time, which have an important effect on the understanding of the quantum size effects of the semiconductor nanocomposites.

In this paper, we report on the nanocomposite preparation of ZnSe nanocrystals in silica gel-glasses. The size and size distribution of ZnSe nanocrystals were both shown by a theoretical analysis based on light diffraction effect, quantum confinement effect, and phonon confinement effect. Theoretical calculations were compared with the experimental results of Raman spectrometry and high-resolution TEM (HRTEM) observations to verify the size estimations deduced from the theoretical calculations.

2 Preparation and characterization

$ZnSe/SiO_2$ nanocomposites were prepared by employing the methods reported by the article [8]. Zinc selenate

M. Wang (✉) · X. Huo · X. Yao · K. Yang · H. Hao · X. Wan
Electronic Materials Research Laboratory,
Key Laboratory of Education Ministry, Xi'an Jiaotong University,
Xi'an 710049, China
e-mail: mqwang@mail.xjtu.edu.cn

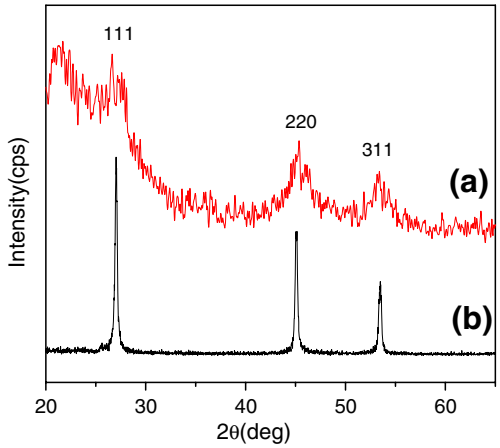

Fig. 1 XRD patterns of $ZnSe/SiO_2$ gel-glass (**a**) and crystalline ZnSe powder (**b**)

($ZnSeO_4$) solution as the dopant phase was introduced to the hydrolyzed solution of tetraethoxysilane (TEOS). We have tried several different strategies to avoid aggregation of ZnSe NCs doped in silica gel-glass. The comparatively effective approaches to avoid the aggregation include (a) delaying the introduction of the dopant phase in order to use the sol–gel matrix as a fixative agent, (b) aging the sol in Petri dishes tightly covered by filter paper to slower the volatilization of the water and alcohol in the sol–gel solution, (c) performing two-step thermal treatments respectively in air and then reductive atmosphere of carbon monoxide just after the formation of the sol–gel, (d) avoiding the diffusion of Se in the gel-glasses with putting some ZnSe powders in tube atmosphere furnace during reductive thermal treatment.

The samples were analyzed by the transmission electron microscopy (Tecnai F30). XRD patterns of the samples were measured with D/max-RB diffractometer using Cu radiation as a source, with voltage 40 kV, current 200 mA, wavelength 0.1532 nm, scanning velocity 10 °C/min. Absorption spectrum is measured by Jasco v-570 spectrometer in the range of 340–800 nm at room temperature. Raman spectrum was performed by an Ar+ laser with the wavelength of 514.5 nm in back scattering at room temperature.

3 Results and discussion

To demonstrate the formation of ZnSe nanocrystals within the gel-glasses, we choose the gel-glasses containing 6% molar ratio of ZnSe dopant as an X-ray diffraction sample. The XRD pattern of crystalline ZnSe powder is also shown in Fig. 1 for comparison. From Fig. 1, the peaks of noncrystalline silica glass and ZnSe can be clearly distinguished. The ZnSe nanocrystals were refined as a zinc-blend structure, while the broadening diffraction peaks are associated with the size reduction to nanoscale regime. The mean size of the ZnSe nanocrystal was estimated by Scherrer formula. It is found that the peak of (220) at $2\theta = 45.2°$ is influenced little by the diffuse of silica and has less measurement error compared with other two peaks. So the peak of (220) is selected to calculate the mean size of ZnSe NCs. With the Gauss fit, the full width at half maximum B is 2.19°, $\theta_B = 22.6°$. Calculated by Scherrer formula, the mean diameter of the nanocrystals is 4.2 nm.

More precise particle size evaluation was performed by HRTEM. The observed samples were prepared by grinding and then milling. Figure 2 shows the HRTEM image of ZnSe NCs in silica gel-glass matrix. It can be seen that ZnSe NCs with well-defined spherical shapes were formed. The corresponding fast Fourier-transform (FFT) of the indicated region was shown in the inset of Fig. 2. The high-resolution image provides insight into the structure details of the ZnSe NCs. The characteristic size of the particles in the 6% sample was about 5 nm. From Fig. 2, the mean size of ZnSe NCs is affected by the concentration doped in silica gel-glass. The lower doping concentration may give rise to the smaller sizes of the NCs. If the ZnSe NCs concentration is low, the particles tend to be very well dispersed, and the NCs embedded in the silica could exhibit narrow size distribution.

Figure 3 shows the absorption spectrum of $ZnSe/SiO_2$ gel-glasses with different molar ratio of ZnSe dopant. The absorption edge of the ZnSe NCs is shifted to higher energies than that of bulk ZnSe (2.58 eV) due to the quantum confinement effects. In addition, as the $ZnSe/SiO_2$ molar ratio decreases, the absorption edge shifts substan-

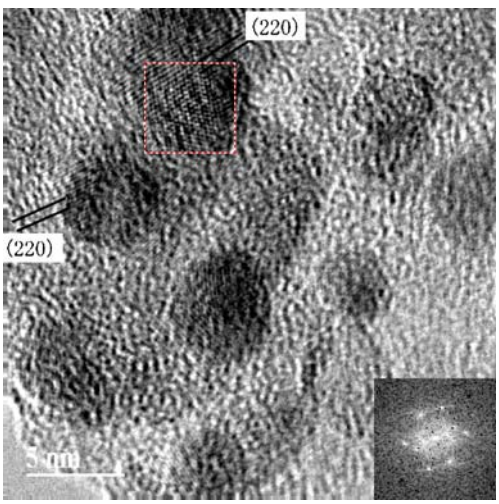

Fig. 2 HRTEM image of the ZnSe NCs doped in silica gel-glass. *Inset* shows the FFT patterns of the corresponding HRTEM image

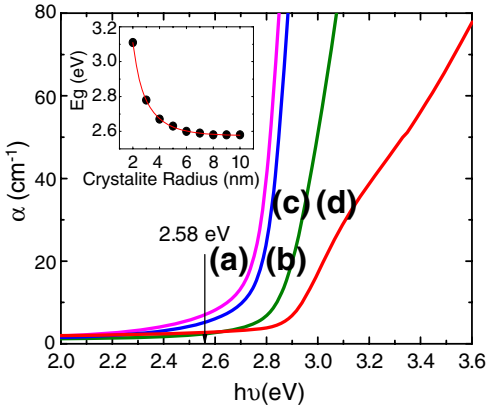

Fig. 3 Optical absorption spectra of ZnSe/SiO_2 molar ratio: (**a**) 6%; (**b**) 4%; (**c**) 2%; (**d**) 1%. *Inset* shows the relationship between size of nanocrystal and the lowest exciton by theory EMA

tially to higher energies, which indicates a decrease of NCs mean size. The absorption of sample a, b and c increases sharply beyond the absorption edge and no feature could be seen at higher photon energies. The absorption spectrum of sample d shows a shoulder around 3.07 eV. Our explanation is that absorption of sample d is small enough to show more fine features. According to the effective mass approximation (EMA), also considering the effect of Coulomb interaction energy, the whole change of transition energy of ZnSe nanocrystals is as follows [9]:

$$E_g = E_{g0} + \frac{\hbar\pi^2}{2R^2}\left(\frac{1}{m_e^*} + \frac{1}{m_h^*}\right) - \frac{1.8e^2}{\varepsilon_2 R} \tag{1}$$

Here, R is the radii of nanocrystal. For ZnSe, dielectric constant ε_2=8.1, electron effective mass m_e^*=0.16m_0, hole effective mass m_h^*=0.7m_0, where m_0 is free electron mass. In the right side of Eq. (1), the first term is the energy gap of bulk ZnSe, E_{g0}=2.58 eV, the second term is the confinement energy, the last term indicates the Coulomb interaction energy. According to Eq. (1), the relation between the lowest exciton transition energy E_g and the radius of ZnSe nanocrystal can be obtained, which is showed in the inset of Fig. 3. When the radius of ZnSe nanocrystal is below 10 nm, the absorption edge shifted toward higher energy with size reduction. The blueshift of absorption edge can be used to judge whether the NCs are in the strongly confined regime.

Figure 4 shows the Raman spectra of the nanocomposite with molar ratio 6% of ZnSe dopant. The peak around 257 cm^{-1} is the first-order longitudinal optical (1LO) phonon Raman spectra of ZnSe NCs doped in silica gel-glass. The asymmetric broadening of 1LO phonon peak was related with the size of the ZnSe nanocrystal by the spatial correlation model [10], or phonon confinement effect. A Gaussian localization factor $\exp(-q^2L^2/4)$ is introduced into the phonon wave function, where L is the correlation length and q is phonon wave vector. The Raman intensity at ω frequency can be written as:

$$I(\omega) \propto \int_0^1 \exp\left(-q^2L^2\right)\frac{d^3q}{\left\{[\omega-\omega(q)]^2+(\Gamma_0/2)^2\right\}} \tag{2}$$

The dispersion relation of optical phonon is derived from a one-dimensional linear chain model [11]:

$$\omega^2(q) = A + \left[A^2 - B(1-\cos q)\right]^{1/2} \tag{3}$$

where two constants A and B are chosen according to the reference [11].

By using Eqs. (2) and (3) and Γ_0=4.8 cm^{-1}, A=3.2×104 cm^{-2}, B=4.5×108 cm^{-4} for ZnSe, the theoretical line shape $I(\omega)$ could be calculated for different values of L. This in turn gives the calculated line width T and ratio T_a/T_b, where T is the full width at half maximum of the line shape, T_a and T_b are the left and the right half widths at half maximum of the line shape, respectively. The predicated relations between L, T_a/T_b and T could be obtained. The fitting value of L to the observed T and T_a/T_b is correspond to 4.2 nm, a value very close to the one obtained by HRTEM analysis. The model also predicts a redshift of 1LO peak as a function of particle size L. But the experiment results for our samples are blueshift, which is different from the redshift predicted by the phonon confinement model. The theory can't explain the Raman spectrum properties of ZnSe NCs properly, there could be some other affections such as surface stress and lattice parameters potty change, which is not clear yet and need further study.

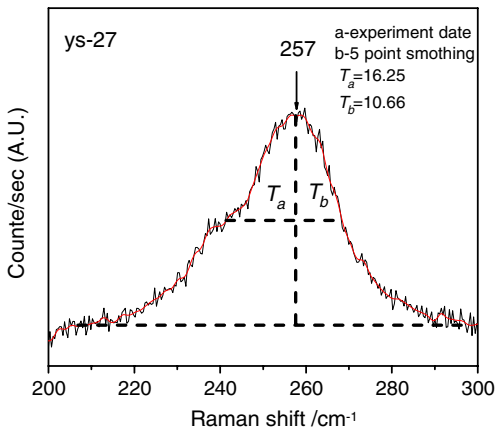

Fig. 4 Raman spectrum of ZnSe nanocrystals doped in gel-glass in the vicinity of the LO phonon

4 Conclusions

The $ZnSeO_4$ solution as dopant phase could be introduced to the hydrolyzed solution of TEOS to get the homogeneously doped sol and the dry gel. A subsequent reductive thermal treatment led to ZnSe nanocrystals in-situ grown in gel-glass and the formation of transparent, homogeneous and yellow color $ZnSe/SiO_2$ gel-glasses. The comparatively effective approaches for avoiding the aggregation of ZnSe NCs doped in silica gel-glass during the preparation process were presented for the first time. The broadening of XRD peaks, the blueshifts of the interband optical absorption edge and the change of Raman spectrum were observed.

Acknowledgements This work was supported by the Ministry of Sciences and Technology of China through the 973-project under grant 2002CB613305, the Nature Science Foundation of Shannxi Province (2003E110) and Xi'an Science and Technology developing Project (GG05040).

References

1. L.L. Beecroft, C.K. Ober, Chem. Mater **9**, 1302 (1997)
2. L.P. Li, G.S. Li, R.L. Smith Jr., H. Inomata, Chem. Mater **12**, 3705 (2000)
3. G. Li, M. Nogami, J. Appl. Phys **75**, 4276 (1994)
4. V.J. Leppert, S.H. Risbud, M.J. Fendorf, Phil. Mag. Lett **5**, 29 (1997)
5. M. Hayashi, T. Iwano, H. Nasu, K. Kamiya, N. Sugimoto, K. Hirao, J. Mater. Res **12**, 2552 (1997)
6. J.C. Jan, S.Y. Kuo, S.B. Yin, W.F. Hsieh, Chinese J. Physiol **39**, 90 (2001)
7. C. Sanchez, B. Lebeau, F. Chaput et al., Adv. Mater **15**, 1969 (2003)
8. M.Q. Wang, Y.P. Wang et al., Chin. Sci. Bull **49**, 747 (2004)
9. L.E. Brus, J. Phys. Chem **80**, 4403 (1984)
10. D. Sarigiannis, J.D. Peck, G. Kioseoglou, A. Petrou, T.J. Mountziaris, Appl. Phys. Lett **80**, 4024 (2002)
11. J. Wang, W.H. Yao, J.B. Wang, H.Q. Sun, X. Wang, Z.L. Peng, Appl. Phys. Lett **62**, 31 (1993)